Inorg. Chem. **2005**, *44*, 4263–4269

Effect of the Semirigid Capping Ligand on the Structure Formation of Cyano-Bridged Bimetallic Assemblies: Syntheses, Crystal Structures, and Magnetic Properties

Xiao-Yan Chen, Wei Shi, Jun Xia, Peng Cheng,* Bin Zhao, Hai-Bin Song, Hong-Gen Wang, Shi-Ping Yan, Dai-Zheng Liao, and Zong-Hui Jiang

Department of Chemistry, Nankai University, Tianjin 300071, People's Republic of China

Received January 21, 2005

The syntheses, crystal structures, and magnetic properties of three novel cyano-bridged bimetallic assemblies, $[Ni(bpm)_2]_3[Co(CN)_6]_2 \cdot 3.5H_2O$ (**1**), $[Co(bpm)_2][Fe(CN)_5NO] \cdot 2H_2O$ (**2**), and $[Co(bpm)_2][Ni(CN)_4]$ (**3**) (bpm = bis(1-pyrazolyl)methane), are reported. Complex **1** crystallizes in the tetragonal space group $P4_32_12$ with $a = 12.800(5)$ Å, $b = 12.800(5)$ Å, $c = 42.80(3)$ Å, $V = 7012(6)$ Å^3, and $Z = 8$. Complex **2** crystallizes in the chiral trigonal space group $P3_221$ with $a = 11.9961(19)$ Å, $b = 11.9961(19)$ Å, $c = 16.062(5)$ Å, $\gamma = 120°$, $V = 2001.7(8)$ Å^3, and $Z = 3$. Complex **1** is a trigonal bipyramidal complex in which three $[Ni(bpm)_2]^{2+}$ units are situated in the equatorial plane and are connected to the two apical $[Co(CN)_6]^{3-}$ units via three N ends of the cyanide groups. Complex **2** possesses a triangular left-handed helical chain structure composed of $[Co(bpm)_2]^{2+}$ linked by $[Fe(CN)_5NO]^{2-}$; the shortest intramolecular Co···Fe distance is 5.162 Å. To the best of our knowledge, this is the first observation of a heteronuclear helical chain structure based on pentacyanonitrosylferrate(II). The structure of complex **3** is roughly determined by X-ray crystallograhy analysis to be a 1D zigzag chain. These structure variations, from a discrete cluster to a 1D helical chain and a 1D zigzag chain, rely on the semirigidity of the capping ligand bpm. Magnetic susceptibility measurements indicate that complex **1** has an intramolecular ferromagnetic interaction ($J = 4.06$ cm^{-1}) between the nickel(II) ions; this is further confirmed by the magnetization measurements. In complexes **2** and **3**, the cobalt(II) ions are located in a moderately strong field.

Introduction

Research in transition metal−cyanide chemistry is experiencing a renaissance because of the novel magnetic properties exhibited by face-centered 3D "Prussian blue" compounds.[1−4] Some exciting results such as long-range magnetic ordering above room temperature have been reported.[2] Recently, zero- and low-dimensional cyano-bridged compounds have drawn our attention as single-molecule magnets and single-chain magnets. However, it is extremely difficult to grow crystals of these cyanide-containing compounds. On the other hand, when we study the magneto-structural relationship of cyanide-based assemblies, which lack solubility because of the strong tendency of cyanides to form three-dimensional networks, the simplest modes possible are needed. Thus, a new effort to prepare cyano-bridged complexes with oligonuclear and low-dimensional structures has been made by introducing capping ligands into the coordination sphere of the cation.[5−8]

* To whom correspondence should be addressed. E-mail: pcheng@nankai.edu.cn. Fax: +86-22-23502458.

(1) Dunbar, K. R.; Heintz, R. A. *Prog. Inorg. Chem.* **1997**, *45*, 283.
(2) Holmes, S. M.; Girolami, G. S. *J. Am. Chem. Soc.* **1999**, *121*, 5593.
(3) Beauvais, L. G.; Long, J. R. *J. Am. Chem. Soc.* **2002**, *124*, 12096.
(4) Sato, O.; Iyoda, T.; Fujishima, A.; Hashimoto, K. *Science* **1996**, *272*, 704.
(5) Kou, H.-Z.; Gao, S.; Ma, B.-Q.; Liao, D.-Z. *Chem. Commun.* **2000**, 713.
(6) (a) Colacio, E.; Ghazi, M.; Stoeckli-Evans, H.; Lioret, F.; Moreno, J. M.; Pérez, C. *Inorg. Chem.* **2001**, *40*, 4876. (b) Van Langenberg, K.; Batten, S. R.; Berry, K. J.; Hockless, D. C. R.; Moubaraki, B.; Murray, K. S. *Inorg. Chem.* **1997**, *36*, 5006. (c) Berlinguette, C. P.; Galán-Mascarós, J. R.; Dunbar, K. R. *Inorg. Chem.* **2003**, *42*, 3416. (d) Van Langenberg, K.; Hockless, D. C. R.; Moubaraki, B.; Murray, K. S. *Synth. Met.* **2001**, *122*, 573.
(7) (a) Shek, I. P. Y.; Wong, W. T.; Gao, S.; Lau, T. C. *New J. Chem.* **2002**, *26*, 1099. (b) Fallah, M. S. E.; Ribas, J.; Solans, X.; Font-Bardia, M. *New J. Chem.* **2003**, *27*, 895. (c) Berlinguette, C. P.; Dragulescu-Andrasi, A.; Sieber, A.; Galán-Mascarós, J. R.; Güdel, H.-U.; Achim, C.; Dunbar, K. R. *J. Am. Chem. Soc.* **2004**, *126*, 6222.
(8) (a) Marvaud, V.; Decroix, C.; Scuiller, A.; Guyard-Duhayon, C.; Vaissermann, J.; Gonnet, F.; Verdaguer, M. *Chem.—Eur. J.* **2003**, *9*, 1678. (b) Marvaud, V.; Decroix, C.; Scuiller, A.; Tuyèras, F.; Guyard-Duhayon, C.; Vaissermann, J.; Marrot, J.; Gonnet, F.; Verdaguer, M. *Chem.—Eur. J.* **2003**, *9*, 1692.

10.1021/ic050099g CCC: $30.25
Published on Web 05/11/2005

Scheme 1

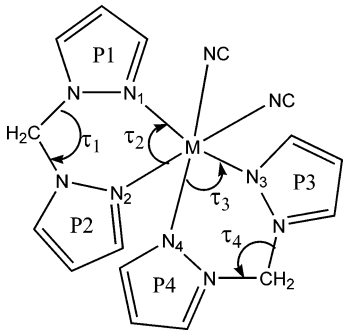

This strategy favors the crystallization of the compounds and the study of the magneto-structural relationship. The capping ligands can control the topology of the metal ions thereby enhancing the solubility of the resulting compounds. For metal ions that have six-coordinate geometry, bis-bidentate- or tetradentate-capped metal centers can receive two additional ligands, such as cyanides or cyanometalates, to form new soluble cyanide-based assemblies with a reduced number of metal−cyano−metal linkages. So far, chelating amines, such as ethylenediamine, 1,3-propylenediamine, or 1,4,8,-11-tetraazacyclotetradecane and *N*,*N*′,*N*″-trimethyl-1,4,7-triazacyclononane, have usually been employed.[7,9−12] Here, we adopt the same capping ligand as used by Murray et al.,[6b] bpm (bis(1-pyrazolyl)methane), which is a bidentate semirigid ligand. $[Ni(bpm)_2]_3[Co(CN)_6]_2\cdot 3.5H_2O$ (**1**), $[Co(bpm)_2][Fe(CN)_5NO]\cdot 2H_2O$ (**2**), and $[Co(bpm)_2][Ni(CN)_4]$ (**3**) have been synthesized using this ligand. As in the case of the pentanuclear cluster $[Ni(bpm)_2]_3[Fe(CN)_6]_2\cdot 7H_2O$,[6b] complex **1** forms an isostructural discrete pentanuclear cluster; each cluster is connected to the neighboring clusters in the crystal lattice via hydrogen bonds from the water molecules to give a complicated three-dimensional network. The same type of cluster has also been reported using other N,N-bidentate ligands, such as tmphen and 2,2′-bipyridine.[6c,d] Magnetic susceptibility measurements indicate that complex **1** has intramolecular ferromagnetic interactions ($J = 4.06$ cm^{-1}) between nickel(II) ions; this is confirmed by the magnetization measurements. In complex **2**, pentacyanonitrosylferrate(II) connects the cobalt(II) ions through cyanide bridges to form a heteronuclear left-handed helical chain. As far as we know, there has been no report of cyanometalate-based helical structures until now. Complex **3** displays a zigzag chain structure. The capping ligand favors the different structures in these lattices because of the semirigidity of bpm (Scheme 1) and the regular variation in the dihedral angle of the two pyrazole rings (P1, P2 or P3, P4) in one bpm ligand, the dihedral angle of the two M-bpm coordinating planes (MN_1N_2 and MN_3N_4), and the $\tau_1-\tau_4$ angles. This leads to the formation of cyanide-bridged complexes with structures ranging from discrete pentanuclear complexes to 1D chains.

Experimental Section

All of the reagents were used as received from commercial suppliers without further purification. The bpm ligand was prepared by the literature method.[14] *Caution!* Perchlorate salts of metal complexes with organic ligands are potentially explosive. Only small amounts of material should be prepared, and these should be handled with caution.

Elemental analyses for C, H, and N were carried out at the Institute of Elemental Organic Chemistry, Nankai University. IR spectra were recorded in KBr disks on a Bruker Tensor 27 infrared spectrophotometer in the 4000−600 cm^{-1} region. The variable-temperature magnetic susceptibilities of crashed single-crystal samples in the temperature range of 2−300 K (**1**) and 5−300 K (**2** and **3**) were measured on a Quantum Design MPMS-7 SQUID magnetometer in a field of 2 T (**1**) and 1 T (**2** and **3**), respectively. Diamagnetic corrections were made with Pascal's constants for all of the constituent atoms.

Synthesis of $[Ni(bpm)_2]_3[Co(CN)_6]_2\cdot 3.5H_2O$ (1). Complex **1** was prepared by the slow diffusion at room temperature in water of bpm (0.018 g, 0.12 mmol) and $Ni(ClO_4)_2\cdot 6H_2O$ (0.022 g, 0.06 mmol) on one side of a U-shaped tube containing silica gel with $K_3[Co(CN)_6]$ (0.013 g, 0.04 mmol) on the other side. After a few weeks, well-shaped blue crystals suitable for X-ray analysis were obtained. Yield: 30%. Anal. Calcd for $C_{54}H_{55}N_{36}O_{3.5}Co_2Ni_3$ (1558.34): C, 41.62; H, 3.56; N, 32.36. Found: C, 41.14; H, 3.31; N, 32.89. IR (KBr, cm^{-1}): 3138, 3125, 2160, 2135, 1634, 1516, 1430, 1397, 1330.

Synthesis of $[Co(bpm)_2][Fe(CN)_5NO]\cdot 2H_2O$ (2). Complex **2** was obtained as yellow crystals in a manner similar to that used to obtain complex **1** except for the use of $Co(ClO_4)_2\cdot 6H_2O$ and $Na_2[Fe(CN)_5NO]\cdot 2H_2O$. Yield: 34%. Anal. Calcd for $C_{19}H_{20}N_{14}O_3CoFe$ (607.27): C, 37.58; H, 3.32; N, 32.29. Found: C, 37.21; H, 3.54; N, 32.76. IR (KBr, cm^{-1}): 3135, 3100, 2190, 2170, 1930, 1655, 1616, 1410, 1360, 1310.

Synthesis of $[Co(bpm)_2][Ni(CN)_4]$ (3). Complex **3** was prepared as pink crystals in a manner similar to that used to obtain complex **1** except for the use of $Co(ClO_4)_2\cdot 6H_2O$ and $Na_2[Ni(CN)_4]$. Yield: 20%. Anal. Calcd for $C_{18}H_{16}N_{12}CoNi$ (518.07): C, 41.73; H, 3.11; N, 32.44. Found: C, 41.36; H, 3.45; N, 32.13. IR (KBr, cm^{-1}): 2160, 2133, 1720, 1685, 1520, 1350.

X-ray Crystallography. Crystals with approximate dimensions of 0.18 × 0.16 × 0.14 and 0.35 × 0.25 × 0.10 mm of complexes **1** and **2**, respectively, were mounted on a glass fiber. Determination of the unit cell and data collection were performed with Mo Kα radiation ($\lambda = 0.71073$ Å) on a BRUKER SMART 1000 diffractometer equipped with a CCD camera. The $\omega-\varphi$ scan technique was employed.

The structures were solved primarily with a direct method and secondarily with Fourier difference techniques. They were refined by the full-matrix least-squares method. The computations were performed with the SHELXL-97 program.[15,16] All non-hydrogen

(9) Kou, H.-Z.; Gao, S.; Zhang, J.; Wen, G.-H.; Su, G.; Zheng, R. K.; Zhang, X. X. *J. Am. Chem. Soc.* **2001**, *123*, 11809.
(10) Lu, T. B.; Xiang, H.; Su, C. Y.; Cheng, P.; Mao, Z. W.; Ji, L. N. *New J. Chem.* **2001**, *25*, 216.
(11) Shores, M. P.; Long, J. R. *J. Am. Chem. Soc.* **2002**, *124*, 3512.
(12) Vostrikova, K. E.; Luneau, D.; Wernsdorfer, W.; Rey, P.; Verdaguer, M. *J. Am. Chem. Soc.* **2000**, *122*, 718.
(13) (a) Kou, H.-Z.; Bu, W. M.; Gao, S.; Liao, D. Z.; Jiang, Z. H.; Yan, S. P.; Fan, Y. G.; Wang, G. L. *J. Chem. Soc., Dalton Trans.* **2000**, 2996. (b) Kou, H.-Z.; Gao, S.; Bai, O.; Wang, Z.-M. *Inorg. Chem.* **2001**, *40*, 6287. (c) Colacio, E.; Domínguez-Vera, J. M.; Lloret, F.; Rodríguez, A.; Stoeckli-Evans, H. *Inorg. Chem.* **2003**, *42*, 6962.
(14) (a) Zhang, L.; Cheng, P.; Tang, L. F.; Weng, L. H.; Jiang, Z. H.; Liao, D. Z.; Yan, S. P.; Wang, G. L. *Chem. Commun.* **2000**, 717. (b) Tang, L. F.; Jia, W. L.; Wang, Z. H.; Wang, J.-T.; Wang, H.-G. *J. Organomet. Chem.* **2002**, *649*, 152.
(15) Sheldrick, G. M. *SHELXS 97, Program for the Solution of Crystal Structures*; University of Göttingen: Göttingen, Germany, 1997.
(16) Sheldrick, G. M. *SHELXL 97, Program for the Refinement of Crystal Structures*; University of Göttingen: Göttingen, Germany, 1997.

Table 1. Data Collection and Processing Parameters for Complexes **1**−**3**

	1	**2**	**3**
formula	$C_{54}H_{55}N_{36}O_{3.5}Co_2Ni_3$	$C_{19}H_{20}N_{14}O_3CoFe$	$C_{18}H_{16}N_{12}CoNi$
fw	1558.34	607.27	518.07
T (K)	293(2)	293(2)	293(2)
cryst syst	tetragonal	trigonal	orthorhombic
space group	$P4_32_12$	$P3_221$	*Cmcm*
a (Å)	12.800(5)	11.9961(19)	14.215(7)
b (Å)	12.800(5)	11.9961(19)	9.376(5)
c (Å)	42.80(3)	16.062(5)	16.615(9)
γ (deg)	90	120	90
V (Å^3)	7012(6)	2001.7(8)	2215(2)
Z	4	3	4
ρ (g/cm^3)	1.476	1.511	1.554
μ (mm^{-1})	1.324	1.214	1.631
θ (deg)	1.90−25.01	1.96−26.40	2.45−25.02
index ranges	$-15 \le h \le 13$	$-15 \le h \le 14$	$-16 \le h \le 15$
	$-15 \le k \le 15$	$-11 \le k \le 15$	$-10 \le k \le 11$
	$-43 \le l \le 50$	$-20 \le l \le 14$	$-16 \le l \le 19$
reflns collected	34850	11474	5630
independent reflns	5981, $R_{int} = 0.1327$	2730, $R_{int} = 0.0278$	1059, $R_{int} = 0.0681$
maximum, minimum transmission	1.000000, 0.621144	1.000000, 0.905697	0.8944, 0.6671
data/restraints/parameter	5981/48/453	2730/0/176	1059/114/114
GOF on F^2	1.120	1.093	0.977
R_1, R_2 [$I > 2\sigma(I)$]	0.0871, 0.1523	0.0298, 0.0756	0.0674, 0.1879
R_1, R_2 (all data)	0.1194, 0.1662	0.0360, 0.0797	0.1026, 0.2080
largest diff. peak and hole (e Å^{-3})	0.697, −0.521	0.557, −0.302	0.990, −0.543

atoms were refined anisotropically. The hydrogen atoms were set in calculated positions and refined as riding atoms with a common fixed isotropic thermal parameter. Unfortunately, high-quality crystals of complex **3** were not obtained. The poor quality of the structure determination is a result of the high disorder of the organic ligand bpm. The present results were obtained from a crystal with approximate dimensions of 0.27 × 0.16 × 0.07 mm. Crystal parameters and structure refinements for complexes **1**−**3** are summarized in Table 1. Selected bond lengths and angles are listed in Table 2.

Results and Discussion

IR Spectra. The most remarkable feature of the IR spectra of complexes **1**−**3** is the presence of two main peaks at 2160 and 2135 cm^{-1} (**1**), 2190 and 2170 cm^{-1} (**2**), and 2160 and 2133 cm^{-1} (**3**). Their significant shift toward higher frequencies, compared with the ν(C≡N) stretching frequencies of the corresponding mononuclear precursors, $K_3[Co(CN)_6]$ (2126 cm^{-1}), $Na_2[Fe(CN)_5NO]\cdot 2H_2O$ (2143 cm^{-1}), and $Na_2Ni(CN)_4$ (2128 cm^{-1}),[17] suggests the occurrence of a bridging cyanide in the compounds. The splitting of ν(C≡N) indicates the formation of M−CN−M′ linkages. The higher frequencies that appear at 2160, 2190, and 2160 cm^{-1} for complexes **1**, **2**, and **3**, respectively, are assigned to the stretching vibrations of the bridging CN. The peaks at 2135, 2170, and 2133 cm^{-1} for complexes **1**, **2**, and **3**, respectively, are a result of the terminal CN stretching vibrations. The strong single peak at 1930 cm^{-1} for complex **2** is assigned to the NO stretching. The absorption peaks at 1400−1800 cm^{-1} are assigned to the stretching frequencies of ν(C−N) in the pyrazole ring. Finally, strong broad absorptions centered at ca. 3400 cm^{-1} in the spectra of complexes **1** and **2** are attributed to the OH stretching of the lattice water molecules involved in hydrogen bonds.

(17) (a) Jain, S. C.; Warrier, A. V. R.; Sehgal, H. K. *J. Phys. C: Solid State Phys.* **1972**, *5*, 1511. (b) McCullough, R. L.; Jones, L. H.; Crosby, G. A. *Spectrochim. Acta* **1960**, *16*, 929.

Table 2. Selected Bond Lengths (Å) and Angles (deg) for Complexes **1** and **2**

1[a]

Co1−C2	1.8748(8)	Ni1−N7	2.0763(10)
Co1−C4	1.8857(12)	Ni1−N11	2.0929(9)
Co1−C3	1.8859(12)	Ni1−N10	2.1167(9)
Co1−C5	1.9126(9)	Ni1−N14	2.1607(18)
Co1−C6	1.9194(9)	Ni2−N2	2.0395(8)
Co1−C1	1.9401(9)	Ni2−N15	2.1288(9)
Ni1−N1	2.0527(9)	Ni2−N18	2.1331(15)
Ni1−N4A	2.0680(16)		
C2−Co1−C4	90.36(4)	N1−Ni1−N4A	91.29(2)
C2−Co1−C3	87.21(5)	N1−Ni1−N7	89.88(2)
C4−Co1−C3	175.51(2)	N4A-Ni1−N7	96.34(2)
C2−Co1−C5	177.17(3)	N1−Ni1−N11	94.20(2)
C4−Co1−C5	90.72(5)	N4A−Ni1−N11	86.26(3)
C3−Co1−C5	91.89(5)	N7−Ni1−N11	175.12(2)
C2−Co1−C6	89.23(3)	N1−Ni1−N10	174.98(2)
C4−Co1−C6	92.83(3)	N7−Ni1−N10	85.79(2)
C3−Co1−C6	90.92(3)	N11−Ni1−N10	90.01(2)
C5−Co1−C6	88.11(3)	N1−Ni1−N14	90.58(2)
C2−Co1−C1	89.83(3)	N7−Ni1−N14	91.26(3)
C4−Co1−C1	88.04(3)	N11−Ni1−N14	86.02(3)
C3−Co1−C1	88.17(3)	N2−Ni2−N2A	89.90(3)
C5−Co1−C1	92.82(3)	N2−Ni2−N15	91.70(2)
C6−Co1−C1	178.72(3)	N2−Ni2−N18	93.05(3)

2[b]

Co1−N1	2.168(2)	Fe1−N8	1.651(4)
Co1−N5B	2.093(2)	Fe1−C9	1.933(3)
Co1−N5	2.093(2)	Fe1−C9A	1.933(3)
Co1−N3	2.146(2)	Fe1−C10	1.937(5)
Co1−N3A	2.146(2)	Fe1−C8	1.939(2)
Co1−N1A	2.168(2)	Fe1−C8A	1.939(2)
N5B−Co1−N5	90.37(14)	N8−Fe1−C9	95.21(12)
N5B−Co1−N3	90.66(10)	C9−Fe1−C9A	169.6(2)
N5−Co1−N3	93.50(9)	N8−Fe1−C10	180.0(3)
N3−Co1−N3A	174.11(14)	C9−Fe1−C10	84.79(12)
N5−Co1−N1A	176.20(10)	N8−Fe1−C8	94.97(9)
N3−Co1−N1A	87.29(9)	C9−Fe1−C8	88.81(11)
N5B−Co1−N1	176.19(10)	C9A-Fe1−C8	90.29(11)
N5−Co1−N1	93.35(9)	C10−Fe1−C8	85.03(9)
N3−Co1−N1	88.29(9)	C8−Fe1−C8A	170.07(19)

[a] A: $y, x, -z$. [b] A: $x - y, -y, -z + {}^1/_3$; B: $y + 1, x - 1, -z$.

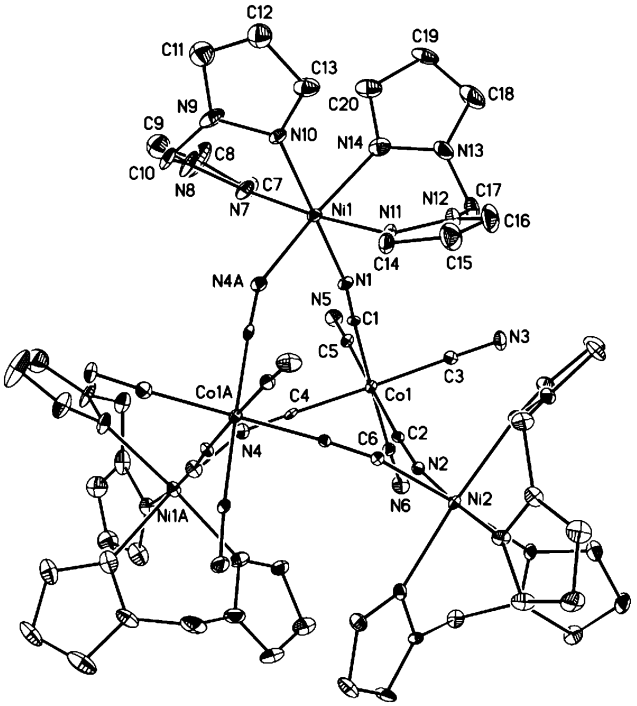

Figure 1. ORTEP drawing of complex **1**. The hydrogen atoms and water molecules are omitted for clarity.

Structure of $[Ni(bpm)_2]_3[Co(CN)_6]_2 \cdot 3.5H_2O$ (1). An ORTEP drawing of the discrete neutral pentanuclear cluster is shown in Figure 1. In this compound, three $[Ni(bpm)_2]^{2+}$ units are situated in the equatorial plane and are connected to the two apical $[Co(CN)_6]^{3-}$ units via the N end of three *fac* CN− ligands. The geometry around the nickel atom is octahedral, with three nitrogen atoms from the bpm ligands (Ni1−N, 2.0763(10) and 2.1167(9) Å) and one nitrogen atom from the cyanide group (Ni1−N1, 2.0527(9) Å) in the equatorial plane. The other two nitrogen atoms from bpm (Ni1−N14, 2.1607(18) Å) and the cyanide group (Ni1−N4A, 2.0680(16) Å) occupy the axial positions with a N14−Ni1−N4A angle of 172.17(2)°. The Ni1 atom is displaced from the mean equatorial plane by 0.0474 Å. Co−C≡N bond angles vary only over a small range of 175.01(5)−177.72(6)°, whereas Ni−N−C angles differ significantly from linearity (156.18(5)−170.55(5)°). The key bridging pathways within each cluster of complex **1** are the cis-disposed Co−C≡N−Ni−N≡C−Co linkages. The average Co···Ni, Co···Co, and Ni···Ni separations within the cluster are 5.0157, 6.402, and 6.733 Å, respectively. The crystal structure of complex **1** is analogous to that of other trigonal bipyramidal compounds with the general formula $\{[Ni(L-L)_2]_3[Fe(CN)_6]_2\}$.[6,12,18]

The presence of water molecules in the structure of complex **1** enables it to form two kinds of hydrogen bonds with the nitrogen atoms of the terminal cyanide ligands (O···N distance, 2.797 and 2.942 Å; N−O−N angle, 95.05°) which results in a complicated three-dimensional network of H-bonded pentanuclear clusters and water molecules (Figure 2). In comparison to Murray's pioneering work[6] with a pentanuclear complex with bpm, the title complex represents a completely different hydrogen-bonded array because of the different number of lattice water molecules.

Structure of $[Co(bpm)_2][Fe(CN)_5NO] \cdot 3H_2O$ (2). X-ray crystal structure analyses reveal that complex **2** crystallizes in the chiral trigonal space group, $P3_221$, and consists of left-handed structures of Co(II) and Fe(II) ions. The surroundings of the metal ions and linkages of complex **2** are illustrated in Figure 3a. Each Co^{2+} center is octahedral and is coordinated by four nitrogen atoms from the bpm ligands (Co−N, 2.146(2) and 2.168(2) Å) and two nitrogen atoms from the cyanide groups (Co−N, 2.093(2) Å). The Co1 atom is displaced from the mean N3N5N1AN3A equatorial plane by 0.0721 Å. As expected, the Fe−C≡N bond angles are almost linear (178.7(2)−180.0(7)°); however, the Co−N≡C bond angles are also linear (170.8(2)°), which is different from that in complex **1**.

The bridging Co−CN−Fe−CN−Co pathway observed here results in a very interesting infinite helical chain running along the crystallographic *c* axis (Figure 3b). The left-handed helix is generated around the crystallographic 3_1 axis with a pitch of 16.062 Å. Notably, each pair of nearly perpendicular bpm ligands bonded to the Co atom points away from the helical axis; this steric orientation leads to the generation of a triangular channel (Figure 3c). The nearest Co···Co and Fe···Fe separations in the polymer are 10.305 and 6.595 Å, respectively. Recently, two three-dimensional chiral networks, $[\{Cr(CN)_6\}(Mn_L\text{-aminoalanine})_3]\cdot 3H_2O$ and $[\{Cr(CN)_6\}(Mn_D\text{-aminoalanine})_3]\cdot 3H_2O$, with triple-helical-strand structure were reported, in which the hexacyanometalate ion utilizes all of its cyanide moieties to connect to the adjacent three triple-helical strands containing Mn(II) ions through cyanide bridges.[19] Notably, the pentacyanonitrosylferrate(II) is a part of the left-handed helical chain in complex **2**. To our knowledge, no helical structures which have cyanide building blocks as parts of the helical structure were reported prior to this observation, although many other helical lattices are known.[20]

Structure of $[Co(bpm)_2][Ni(CN)_4]$ (3). The rough X-ray diffraction analyses reveal that complex **3** possesses a 1D zigzag chain structure. The Co atom, with a coordination environment similar to that in complex **2**, is bridged by the cyanide groups from $[Ni(CN)_4]^{2-}$. The nearest Co···Ni distance along the chain is 4.991 Å (Figure 4). Unfortunately, two bpm ligands chelating to the Co atom are highly disordered which made the crystal analyses difficult (see Supporting Information).

By comparing the crystal structures of complexes **1**, **2**, and **3**, we found that the capping ligand, bpm, plays an important role during structure formation. A summary of the main structural features is given in Table 3. The differences in the structural parameters result from the semirigidity of the bpm ligand. With the increasing dihedral angle of the P1 and P3 pyrazole rings and the decreasing dihedral angle of the MN_1N_2 and MN_3N_4 plane, the steric hindrance of M

(18) Dey, S. K.; Bag, B.; Abdul Malik, K. M.; El Fallah, M. S.; Ribas, J.; Mitra, S. *Inorg. Chem.* **2003**, *42*, 4029.
(19) Imai, H.; Inoue, K.; Kikuchi, K.; Yoshida, Y.; Ito, M.; Sunahara, T.; Onaka, S. *Angew. Chem., Int. Ed.* **2004**, *43*, 5618.
(20) For examples, see: (a) Masood, M. A.; Enemark, E. J.; Stack, T. D. P. *Angew. Chem., Int. Ed.* **1998**, *37*, 928. (b) Mizukami, S.; Houjou, H.; Nagawa, Y.; Kanesato, M. *Chem. Commun.* **2003**, 1148.

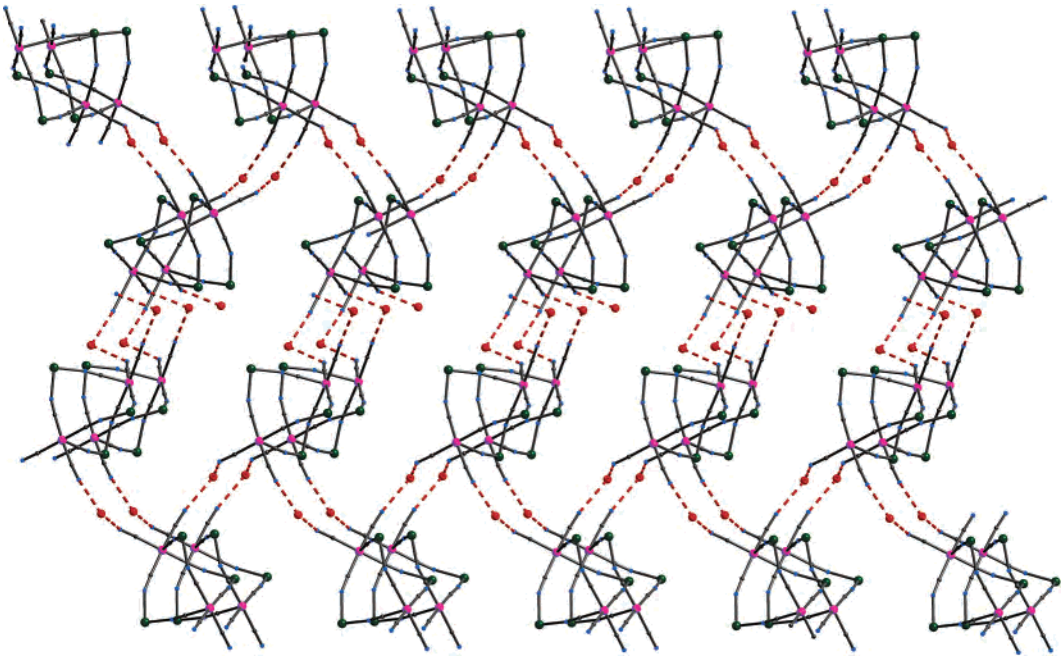

Figure 2. Three-dimensional network formed via hydrogen bonds viewed along the *a* axis. Ni, green; Co, purple; O, red; H-bond, dashed red line.

(M = Ni for **1**, Co for **2** and **3**) decreases accordingly which accounts for the structure transformation from a pentanuclear core (**1**) to a 1D helical chain (**2**) to a 1D zigzag chain (**3**).

Magnetic Properties of $[Ni(bpm)_2]_3[Co(CN)_6]_2\cdot 3.5H_2O$ (1). With regard to the diamagnetic nature of hexacyanocobaltate(III), the magnetic studies allow the evaluation of the Ni−Ni interaction through the long diamagnetic −NC−Co−CN− bridge (more than 10 Å) between the nearest neighbors. The effective magnetic moment of complex **1** at room temperature (Figure 5), 4.88 μ_B, is close to the theoretical value of 4.90 μ_B expected for three isolated nickel(II) ions with $g = 2.0$. The μ_{eff} value gradually increases with decreasing temperature up to the maximum value of 6.28 μ_B at 11 K, and then, below this temperature, the value decreases. This curve is in agreement with ferromagnetic coupling between the nearest nickel ions through the −NC−Co−CN− bridge, which is proposed to occur by a σ-superexchange pathway between the nearest Ni(II) ions through the empty d_σ orbital of the Co(III) ion.[21] The intermolecular interactions, the single-ion zero-field splitting, or both cause a rapid low-temperature decrease in μ_{eff}. The system is treated with a trinuclear approach. Heisenberg exchange theory was utilized, where the Hamiltonian was employed (eq 1)

$$H = -2J(S_1S_2 + S_1S_3 + S_2S_3) \quad (1)$$

The temperature dependence of the magnetic susceptibilities was calculated using the equation derived from the above Hamiltonian operator (eq 2). A temperature independent susceptibility term ($N\alpha$) was also included and set as 2.0×10^{-4} cm^3 mol^{-1}. Then a molecular field approximation (eq 3) was used to modify the intermolecular interaction (zJ') to give the final susceptibility equation of the system.[22]

$$\chi_{Ni} = \frac{Ng^2\beta^2}{kT}\left[\frac{28 + 20\exp(-6J/kT) + 6\exp(-10J/kT)}{7 + 10\exp(-6J/kT) + 9\exp(-10J/kT) + \exp(-12J/kT)}\right] + N\alpha \quad (2)$$

$$\chi_M = \chi_{Ni}/[1 - \chi_{Ni}(2zJ'/Ng^2\beta^2)] \quad (3)$$

The best fit to the magnetic susceptibility data yielded $g = 2.10$, $J = 4.06$ cm^{-1}, $zJ' = -0.31$ cm^{-1}, and the agreement factor $R = 1.1 \times 10^{-3}$ ($R = \sum[(\chi_M)^{bs} - (\chi_M)^{calc}]^2/[(\chi_M)^{bs}]^2$). The field dependence of the reduced magnetization (0−7 T) is measured at 1.84 K. The magnetization tends to be 5.7 $N\beta$, which is close to the expected $S = 3$ for the three-Ni(II) system. The experimental values are higher than those calculated by the Brillouin functions for three isolated centers with $S = 1$. This feature agrees with the global weak ferromagnetic coupling within the three nickel(II) ions.[23] The origin of the ferromagnetic interaction may be the result of a σ-superexchange between the nearest nickel(II) ions ($t_{2g}^6e_g^2$) through the empty d_σ orbital of the cobalt(III) ion (t_{2g}^6). On the basis of this fact, an electron spin of the same sign as that of the unpaired electron on the d_z^2 orbital (paramagnetic Ni^{II}) is polarized on the d_z^2 orbital (diamagnetic Co^{III}) through the filled orbital of the cyanide bridge (the *z* axis is taken along the Ni−C≡N−Co linkage) resulting in a ferromagnetic interaction between the nearest paramagnetic nickel(II) ions.[21,24]

Magnetic Properties of $[Co(bpm)_2][Fe(CN)_5NO]\cdot 2H_2O$ (2). The plots of χ_M and μ_{eff} versus *T* are shown in Figure 6.

(21) Kou, H. Z.; Tang, J. K.; Liao, D. Z.; Gao, S.; Cheng, P.; Jiang, Z. H.; Yan, S. P.; Wang, G. L.; Chansou, B.; Tuchagues, J. P. *Inorg. Chem.* **2001**, *40*, 4839.

(22) O'Connor, C. J. *Prog. Inorg. Chem.* **1982**, *29*, 203.

(23) Wang, L. Y.; Zhao, B.; Zhang, C. X.; Liao, D. Z.; Jiang, Z. H.; Yan, S. P. *Inorg. Chem.* **2003**, *42*, 5804.

(24) Goodenough, J. B. *Phys. Rev.* **1955**, *100*, 564.

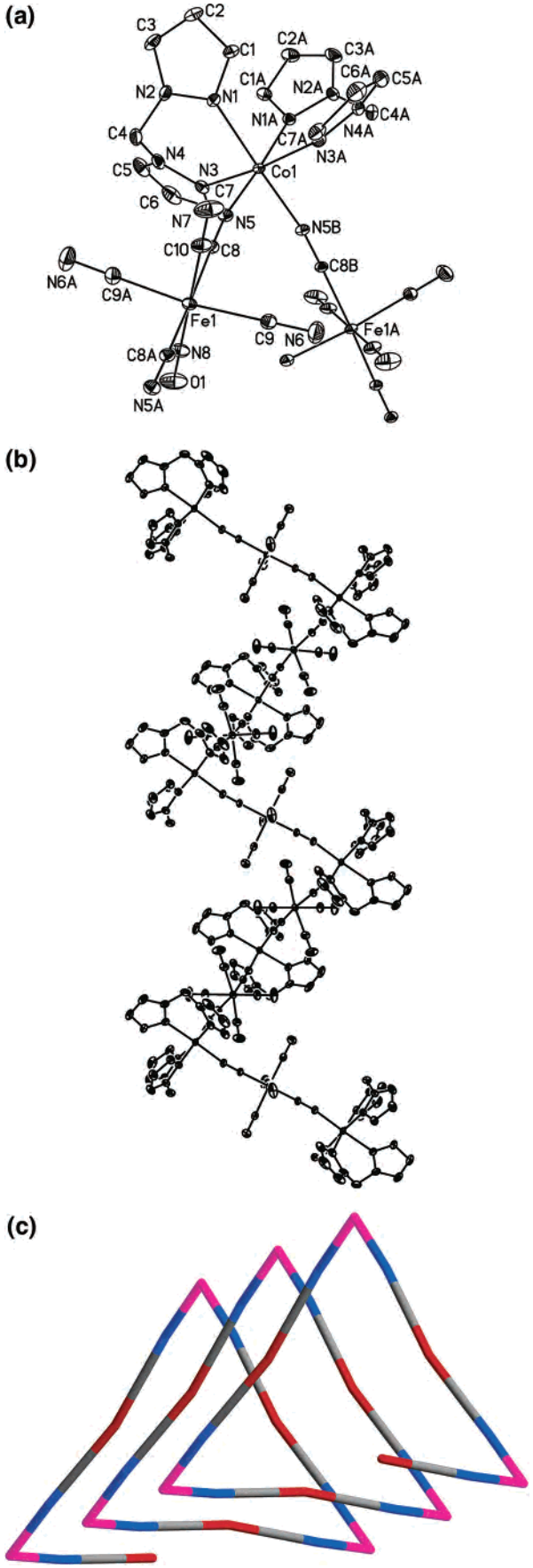

Figure 3. (a) ORTEP drawing of complex **2**, (b) view of the left-handed 3_1 helical chain, and (c) schematic view of the helical chain. Fe, red; Co, purple; C, gray; N, blue.

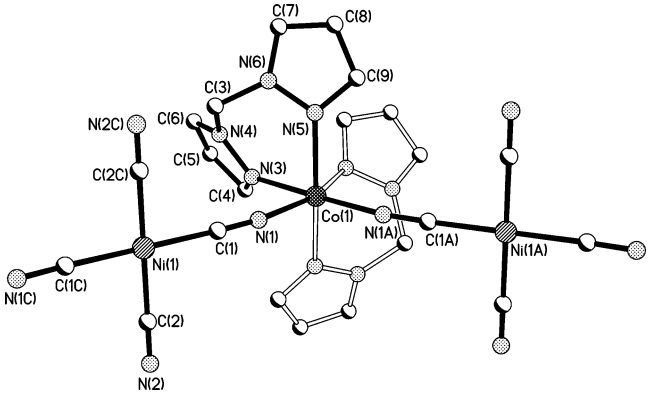

Figure 4. Structure motif of complex **3**. The hydrogen atoms are omitted for clarity.

Table 3. Selected Structural Parameters of $[M(bpm)_2]^{2+}$ in Complexes **1**−**3**

	1	**2**	**3**
$(P1, P2)_{\text{dihedral angle}}$ (deg)	118.3	123.8	115.5
$(P3, P4)_{\text{dihedral angle}}$ (deg)	65.5	56.2	53.4
$(P1, P3)_{\text{dihedral angle}}$ (deg)	70.9	90	107.6
$(MN_1N_2, MN_3N_4)_{\text{dihedral angle}}$ (deg)	87.0	82.9	70.6
τ_1 (deg)	110.17(18)	112.0(2)	109.47(8)
τ_2 (deg)	85.79(2)	88.29(9)	88.83(8)
τ_3 (deg)	86.02(3)	88.29(9)	78.27(4)
τ_4 (deg)	111.26(7)	112.0(2)	109.75(12)

The value of the effective magnetic moment (μ_{eff}) at 300 K is 4.59 μ_B. This value is larger than the spin-only value of high-spin cobalt(II) (3.87 μ_B, $\mu_{so} = [4S(S+1)]^{1/2}$, $S = 3/2$) but close to the value expected when the spin momentum and the orbital momentum exist independently (5.20 μ_B, $\mu_{LS} = [L(L+1) + 4S(S+1)]^{1/2}$, $L = 3$, $S = 3/2$). This indicates a contribution of the orbital momentum typical for the $^4T_{1g}$ ground state. As we know, high-spin octahedral Co^{II} with a $^4T_{1g}$ ground state exhibits unquenched spin−orbital coupling in addition to zero-field splitting, which dominates in the low-temperature region. Unfortunately, no expressions account for both factors simultaneously.[25−27]

The μ_{eff} value continuously decreases from room temperature to 3.89 μ_B at 5.0 K. The χ_M value starts at 0.00886 $cm^3\ mol^{-1}$ at room temperature and increases in a uniform way to 0.37 $cm^3\ mol^{-1}$ at 5 K. The absence of a maximum

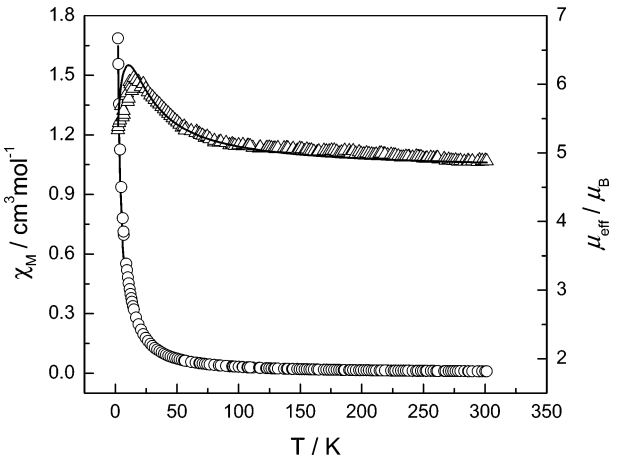

Figure 5. Plots of χ_M (○) and μ_{eff} (△) versus the temperature for complex **1**. The solid line represents the theoretical curve with the best-fit parameters.

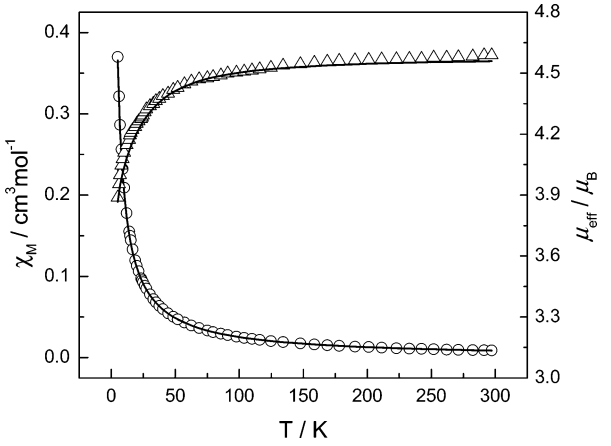

Figure 6. Plots of χ_M (○) and μ_{eff} (△) versus the temperature for complex **2**. The solid line represents the theoretical curve with the best-fit parameters.

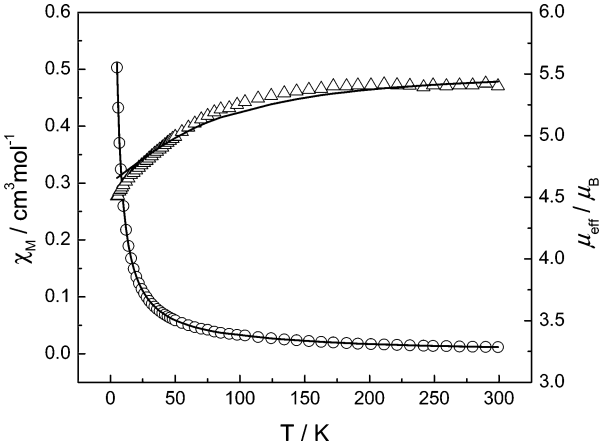

Figure 7. Plots of χ_M (○) and μ_{eff} (△) versus the temperature for complex **3**. The solid line represents the theoretical curve with the best-fit parameters.

in the χ_M curve may indicate that the possible antiferromagnetic coupling is very weak.[25]

We tried to fit the data for the mononuclear Co(II) complex with the following equation (eq 4) for spin−orbital coupling, calculating the λ value and A parameter which gives the measurement of the crystal field strength to the interelectronic repulsions ($x = \lambda/k_BT$, k represents the electron delocalization).[26]

$$\chi_{Co} = \frac{N\beta^2}{3kT}\left[\frac{7(3-A)^2x}{5} + \frac{12(A+2)^2}{25A} + \left\{\frac{2(11-2A)^2x}{45} + \frac{176(A+2)^2}{675A}\right\}\exp\left(-\frac{5Ax}{2}\right) + \left\{\frac{(A+5)^2x}{9} - \frac{20(A+2)^2}{27A}\right\}\exp(-4Ax)\right] / \left\{\frac{x}{3}\left[3 + 2\exp\left(-\frac{5Ax}{2}\right) + \exp(-4Ax)\right]\right\} \quad (4)$$

The molecular field approximation was further considered (eq 5). The best fit (as shown in Figure 6) was obtained with values of $A = 1.31$, $\lambda = -154$ cm^{-1} (λ is the spin−orbital coupling constant, $\lambda = -176.0$ cm^{-1} is the free-ion value), $g = 2.18$, $zJ' = -0.15$ cm^{-1} ($A = 1.5$ is the weak field limit and $A = 1.0$ is the strong field limit), and the agreement factor $R = 9.1 \times 10^{-5}$.

$$\chi_M = \chi_{Co}/[1 - \chi_{Co}(2zJ'/Ng^2\beta^2)] \quad (5)$$

The fitting results indicate that the surrounding of Co(II) in complex **2** is a moderately strong field state and a slightly distorted octahedral arrangement which is consistent with the crystal structure.

Magnetic Properties of $[Co(bpm)_2][Ni(CN)_4]$ (3). The magnetic behavior of complex **3** is similar to that of complex **2**. Therefore, the data for complex **3** were fitted with eq 4 (with $x = \lambda/kT$) for spin−orbital coupling. The molecular field approximation was further considered and the magnetic susceptibility was illustrated in eq 5. The best fit (as shown in Figure 7) was obtained with values of $A = 1.29$, $\lambda = -163$ cm^{-1}, $g = 2.21$, $zJ' = -0.5$ cm^{-1}, and the agreement factor $R = 1.71 \times 10^{-3}$. The above results indicate that, in complex **3**, Co(II) is in a moderately strong field with a slightly distorted octahedral geometry, which is consistent with the crystal structure.

Conclusion

In summary, the employment of bpm, which may block four of the coordination sites of the transition metal ion, allows the syntheses of one pentanuclear cluster $[Ni(bpm)_2]_3[Co(CN)_6]_2\cdot 3.5H_2O$ (**1**), one 1D left-handed helical chain $[Co(bpm)_2][Fe(CN)_5NO]\cdot 2H_2O$ (**2**), and one 1D zigzag chain $[Co(bpm)_2][Ni(CN)_4]$ (**3**) with the cyanometalate linking the $M(bpm)_2^{2+}$ fragment. Remarkably, complex **2** is the first example of a left-handed helical chain with cyanide linkages, which may lead to the production of innovative materials with available magneto-optical properties related to switching functions. The semirigidity of the bpm ligand plays an important role in the formation of the structure of these lattices. This approach could explore other novel interesting cyano-bridged assemblies. The magnetic properties agree with these features. Complex **1** shows weak ferromagnetic coupling between Ni(II) ions, while in complexes **2** and **3**, Co(II) is located in a moderately strong field with a slightly distorted octahedral geometry.

Acknowledgment. This work was supported by the National Natural Science Foundation of China (Grants 90101028 and 20425103).

Supporting Information Available: Crystallographic data in cif format. This material is available free of charge via the Internet at http://pubs.acs.org. CCDC-248966 for complex **1** and CCDC-209039 for complex **2** contain the supplementary crystallographic data for this paper. These data can be obtained free of charge via www.ccdc.cam.ac.uk/conts/retrieving.html (or from the Cambridge Crystallographic Data Center, 12 Union Road, Cambridge CB2 1EZ, UK; fax (+44) 1223-336-033; or e-mail deposit@ccdc.cam.ac.uk).

IC050099G

(25) Hiller, W.; Strahle, J.; Datz, A.; Hanack, M.; Hatfield, W. E.; ter Haar, L. W.; Gutlich, P. *J. Am. Chem. Soc.* **1984**, *106*, 332.
(26) Raebiger, J. W.; Manson, J. L.; Sommer, R. D.; Geiser, U.; Rheingold, A. L.; Miller, J. S. *Inorg. Chem.* **2001**, *40*, 2578.
(27) (a) Chen, X. Y.; Zhao, B.; Cheng, P.; Ding, B.; Liao, D. Z.; Jiang, Z. H.; Yan, S. P. *Eur. J. Inorg. Chem.* **2004**, 562. (b) Hu, X. X.; Xu, J. Q.; Cheng, P.; Chen, X. Y.; Cui, X. B.; Song, J. F.; Yang, G. D.; Wang, T. G. *Inorg. Chem.* **2004**, *43*, 2261. (c) Sun, J. S.; Zhao, H.; Ouyang, X.; Clérac, R.; Smith, J. A.; Clemente, J. M.; Gómez-Garcia, C.; Coronado, E.; Dunbar, K. R. *Inorg. Chem.* **1999**, *38*, 5841.